Citrullination of glucokinase linked to autoimmune diabetes

Mei-Ling Yang[1], Sheryl Horstman[2], Renelle Gee[1], Perrin Guyer[2], TuKiet T. Lam[3,4], Jean Kanyo[4], Ana L. Perdigoto[5], Cate Speake[2], Carla J. Greenbaum[2], Lut Overbergh[6], Richard G. Kibbey[5,7], Kevan C. Herold[5,8], Eddie A. James[2], and Mark J. Mamula[1]¶

[1]Section of Rheumatology, Allergy and Clinical Immunology, [5]Section of Endocrinology, Department of Internal Medicine, [3]Department of Molecular Biophysics & Biochemistry, and [7]Department of Cellular & Molecular Physiology, [8]Department of Immunobiology, Yale University, New Haven, CT, USA

[2]Translational Research Program, Benaroya Research Institute at Virginia Mason, Seattle, WA, USA

Yale University, New Haven, CT, USA.

[4] Keck MS & Proteomics Resource, WM Keck Foundation Biotechnology Resource Laboratory, New Haven, CT, USA.

[6]Laboratory for Clinical and Experimental Endocrinology, KU Leuven, Leuven, Belgium

¶Correspondence: Mark J. Mamula, Yale University, P.O. Box 208031,

300 Cedar Street, New Haven, CT 06520-8031.

E-mail address: mark.mamula@yale.edu.

Abbreviations: T1D; Type 1 diabetes, PTMs; post-translational modifications, glucokinase; GK

Abstract

Inflammation, including reactive oxygen species and inflammatory cytokines in tissue microenvironments amplify the appearance of various post-translational modifications (PTMs) of self-proteins. Previously, a number of PTMs have been identified as autoimmune biomarkers in the initiation and progression of Type 1 diabetes (T1D). Herein, we have identified the citrullination of glucokinase (GK) as a result of inflammation, triggering autoimmunity and affecting its biological functions. Glucokinase is predominantly expressed in hepatocytes to regulate glycogen synthesis, and in pancreatic beta cells, where it acts as a glucose sensor to initiate glycolysis and insulin signaling. Herein, we demonstrate that glucokinase is citrullinated in inflamed non-obese diabetic (NOD) islets as well as in human GK. Autoantibodies against both native and citrullinated GK arise in both spontaneous human T1D and murine models. Likewise, autoreactive $CD4^+$ T cells to both native and citrullinated glucokinase epitopes are present in the circulation of T1D patients. Finally, citrullination alters GK biologic activity and suppresses glucose-stimulated insulin secretion. Our studies define glucokinase as a T1D biomarker, providing new insights into altering glucose metabolism, creating neoautoantigens, and better define the broad impact of PTMs on the tissue pathology of T1D.

INTRODUCTION

Glucokinase (GK, hexokinase IV; EC 2.7.1.2) is one of four isoenzymes of the hexokinase family. Glucose homeostasis in humans is highly regulated by the activity of glucokinase, catalyzing glucose phosphorylation, the first and rate-limiting step of glycolysis in the liver and pancreas [1]. More than 600 mutations of the human glucokinase gene have been described. The majority of these mutations result in reduced glucokinase enzyme activity in pancreatic β-cells and in hepatocytes [2]. As previously described, patients with maturity onset diabetes of the young (MODY) is linked to specific mutations of the glucokinase gene, classified as MODY2 [3, 4]. Thus, glucokinase in particular has been considered as a potential therapeutic target for patients with various forms of diabetes. Since 2008, clinical trials of glucokinase activators have been investigated in patients with type 2 diabetes (T2D), including piragliatin, MK-0941, AZD1656 [5] and dorzagliatin [6]. In contrast to T2D and monogenic diabetes, much less is known regarding the role of glucokinase in autoimmune type 1 diabetes (T1D).

T1D is characterized as an insulin-dependent glucose metabolic disorder arising from inflammation of the pancreatic islets and amplified by autoimmune B and T lymphocyte responses. Besides the role of infiltrating leukocytes into the pancreatic microenvironment, local inflammatory cytokines and reactive oxygen also amplify post-translational protein modifications (PTMs), including deamidation, oxidation, carbonylation and citrullination, that are capable of compromising immune tolerance [7]. Citrullination is an inflammation-dependent process and has been identified in the variety of inflamed tissues and studied extensively as biomarkers of rheumatoid arthritis (RA) [8]. Anti-cyclic citrullinated peptide antibodies (anti-CCP) arise early in RA, correlate with disease severity, and are now routinely used for the diagnosis of RA [9]. T cell recognition of citrullinated epitopes from joint-associated proteins is

also associated with RA [10, 11, 12, 13] . An emerging group of PTM biomarkers important in T1D has been identified including islet cell autoantigen 69 (ICA69), insulin, glutamic acid decarboxylase 65 (GAD65), islet antigen-2 (IA-2) and zinc transporter 8 (ZnT8). Recently, both citrullinated-78-kDa glucose-regulated protein (GRP78) and -GAD65 were found to elicit vigorous B and T cell autoimmune responses in both models of human T1D and NOD murine disease, respectively [14, 15, 16].

Citrullinated proteins are the product of the conversion of peptidylarginine to peptidylcitrulline, which is catalyzed by peptidylarginine deiminases (PADs) in the presence of Ca^{++} [17]. It is well recognized that PAD enzyme levels are increased and associated with tissue inflammation [18]. Five PAD isoenzymes exist in mammals, PAD 1-4 and 6. Among these, PAD2 is widely expressed in different tissues such as brain, spinal cord, spleen, pancreas, bone marrow, skeletal muscle but not detected in liver, kidney and testis [19, 20]. PAD2 expression and activity is increased in synovial fluid from anti-CCP positive RA patients and positively correlated with disease activity [15, 21]. Relevant to T1D, transcriptomic and proteomic profiling demonstrates that PAD2 is highly expressed in prediabetic nonobese diabetes (NOD) islets (2-3 weeks old) compared to age-paired nonobese diabetes-resistant (NOR) and C57Bl/6 islets [22]. In this work, we report that glucokinase undergoes citrullination almost exclusively in the pancreas, not in the liver from NOD mice, even though GK expression is significantly higher in liver. Citrullination alters the enzyme kinetics of pancreatic glucokinase and PAD2/PAD4 inhibitor partially restores impaired insulin secretion mediated by pro-inflammatory cytokines. Our data suggest that citrullination of glucokinase breaks B and T cell tolerance as well as be a marker of beta cell dysfunction of glucose sensing and insulin release in the progress of autoimmune diabetes.

Moreover, the observations support a potential therapeutic strategy of inhibiting PAD enzymes for T1D.

RESULTS

Glucokinase citrullination in inflamed islets from NOD mice and inflammatory stressed-beta cells.

We first performed immunohistochemistry staining and confocal microscope to examine if protein citrullination is increased in islets from the spontaneous NOD murine model of T1D. NOD mice develop hyperglycemia, insulitis, and lymphocyte infiltration of the pancreatic islets as one model of human T1D. Protein citrullination in islets is present already in 3.5 week old NOD mice and increases in staining intensity with increasing age of the mice (Fig. 1a). Citrulline staining coincided with insulitis, as confirmed by hematoxylin–eosin (H&E) staining and anti-CD3 staining from 16 week old NOD mice (Fig. 1b). Protein citrullination is not detected in liver and pancreas extracts from age matched C57Bl/6 mice or in NOD liver, but is significantly present in NOD pancreas (Fig. 1c). PAD treated human GK served as a citrulline staining control.

Glucokinase is the primary glucose sensor since the small fluctuations of its enzyme activity alter the threshold of glucose-stimulated insulin secretion in pancreatic β-cells [1, 23]. In liver, the major role of glucokinase is to regulate the glycogen synthesis. As previously reported [24] and confirmed here, GK levels are expressed in significantly higher levels relative to total protein in liver compared to pancreas from both C57Bl/6 and NOD mice (Fig. 1d). We next immunoprecipitated GK with specific antibody to confirm GK citrullination in NOD pancreas. As expected, we captured significantly more glucokinase from NOD liver extracts compared to

pancreas from 16 week old NOD mice (Fig. 1e). In contrast, the citrullinated glucokinase signal is significantly increased in pancreas compared to liver from NOD mice (Fig. 1e). These data suggest that little overall GK citrullination occurs in the liver, while significant pancreatic GK citrullination arises in the same NOD mouse as disease progresses.

To assess whether inflammation triggers GK citrullination in insulin secreting β-cells, a cocktail of proinflammatory cytokines (rmIFNγ and rhIL-1β) were used to model the insulitis using rat insulinoma cell line, INS-1 cells which displays the key characteristics of pancreatic β cells. The level of protein citrullination was increased in cytokine treated INS-1 cells over time (12, 24 or 48 hours) by immunofluorescence and by flow cytometry (supplementary Fig. 1a, 1b, respectively). As expected, GK^+/$citrullination^+$ populations of INS-1 cells was also increased after cytokine treatment compared to untreated cells in a time dependent manner (supplementary Fig.1 c). Finally, cytokine triggered glucokinase citrullination in INS-1 cells was confirmed by immunoprecipitation with anti-glucokinase and immunoblot with anti-peptidyl-citrulline (supplementary Fig.1d). Collectively, these results illustrate overall pancreatic citrullination and that citrullination of GK can be specifically amplified by inflammatory cytokines in tissue and cell based systems.

Autoantibodies against glucokinase and citrullinated glucokinase arise in both murine and human models of T1D.

We next determined if citrullinated GK may be a neoantigen in triggering autoimmunity in T1D. NOD mouse serum recognized both rhGK and PAD-treated rhGK proteins by immunoblot, while serum from control B10.BR mice did not (Fig. 2a). We next examined IgG autoantibodies to both GK and citrullinated GK by solid phase immunoassay (ELISA) in serum

of NOD mice. Anti-GK and anti-citrullinated-GK IgG titers were significantly higher in both pre-diabetic NOD mice (n=78) and diabetic NOD mice (n=16; blood glucose content greater than 250 mg/dl) compared to control, age matched B10.BR mice (n=52) (Fig. 2b). Subdividing the samples by age groups show that anti-GK and anti-citrullinated-GK IgG arises early in NOD mice, already at 4-6 weeks of age, and before the onset of hyperglycemia. The autoantibody titers against GK and citrullinated GK continue to increase up to 20 week old NOD mice (Supplementary Fig. 2a & b).

To assess B cell reactivity against citrullinated GK and its native counterpart in patients with T1D, serum from patients with T1D (n=55) and healthy control subjects (n=18) were examined by ELISA. As shown in Fig. 2c, patients with T1D had significantly higher anti-GK and anti-citrullinated-GK IgG titer compared to healthy subjects. Other established autoantibodies were also screened within the same set of human serum - including anti-insulin, anti-GAD65, anti-IA2 and anti-ZnT8. Interestingly, anti-GK and anti-citrullinated-GK antibodies correlated positively with anti-ZnT8. There is a biological and metabolic link between zinc ion transport and insulin secretion because mature insulin is stored in the form of Zn-containing hexamers. However, anti-citrullinated-GK antibodies correlated negatively with anti-insulin (Supplementary Table 1).

CD4+ T cells specific for citrullinated glucokinase epitopes are present in the circulation of T1D patients.

We next investigated whether glucokinase peptides are recognized by autoreactive CD4 T cells in patients with T1D. A discrete number of HLA class II haplotypes are highly associated with T1D susceptibility. In particular, HLA-DRB1*04:01 (DR0401), DQA1*03:01-DQB1*0302 (DQ8), HLA-DRB1*03:01 (DR0301) and DQA1*05:01-DQB1*02:01 (DQ2),

confer high risk with about 80-90% of T1D patients carrying at least one of these risk alleles [25]. Prior studies documented that citrullination can enhance peptide binding to DR0401, generating GAD65 neo-epitopes [26]. Therefore, we sought to identify glucokinase sequences that can be bound and presented by DR0401 by scoring all possible nine amino acid motifs within GK using a previously published algorithm [13, 27]. For these predictions, Arg residues that were shown by the mass spectrometry data (Fig. 5b) set to be accessible for modification by PAD enzyme were replaced by citrulline. A total of 38 peptides were synthesized and their binding to recombinant DR0401 protein was assessed using a competition assay [13, 26]. Nine candidate peptides that bound to DR0401 with appreciable affinity (Supplementary Table 2). We then produced DR0401 tetramers for all of those peptides and used these to investigate the ability of each peptide to elicit $CD4^+$ T cell responses *in vitro*. PBMCs from subjects with T1D were stimulated with pools of glucokinase peptides for two weeks, and subsequently stained with the corresponding individual tetramers, revealing five peptides that elicited detectable populations of tetramer-positive T cells in multiple subjects (Supplementary Fig. 3). The sequences of these immunogenic peptides and their predicted motifs are summarized in Table 1. Tetramer-positive T cell clones were isolated for all of those peptides, further confirming T cell recognition of these candidate epitopes (Supplementary Fig. 4).

Among the five immunogenic peptides, three had an Arg residue within the predicted minimal motif (GK 266, GK 270, and GK346) but only one of these, GK residue 358, was shown to be citrullinated. To investigate whether citrullination influenced the binding of these glucokinase epitopes, we compared the HLA binding of citrulline and Arg containing versions of these peptides (Supplementary Table 3). The results indicated that citrullination did not enhance

or alter binding for any of the peptides, which implies that the citrulline/Arg are not T cell contact residues.

To enumerate glucokinase-reactive T cells in human subjects, we applied a direct tetramer enrichment approach [28] to measure their frequency in the peripheral blood of subjects with T1D and HLA matched controls. We labeled individual specificities with PE, PE-CF594, or PE-Cy5 labeled tetramers, staining two separate aliquots of cells to assess the five glucokinase epitopes simultaneously (representative results shown in Supplementary Fig. 5). Some glucokinase-reactive $CD4^+$ T cells were present in controls. However, the combined frequency of glucokinase-reactive $CD4^+$ T cells in subjects with T1D was significantly higher than in controls ($p=0.0007$) (Fig. 3a). Utilizing CD45RA and CCR7 as markers to distinguish antigen-experienced ($CD45RA^-$) versus naïve T cells ($CD45RA^+CCR7^+$), healthy subjects tended to have a higher proportion of glucokinase-reactive T cells that were naïve than subjects with T1D ($p=0.06$) (Fig. 3b). Thus, subjects with established T1D had significantly greater numbers of glucokinase-reactive $CD4^+$ T cells than controls and their glucokinase-reactive T cells tended to show increased signs of antigen exposure. Considering individual specificities, only GK 346 specific T cells were significantly more frequent in subjects with T1D than in controls ($p=0.0004$), but GK 199 and GK 270 also trended toward trended toward having higher frequencies in subjects with T1D ($p=0.08$ and $p=0.09$, respectively) (Fig. 3c). We expressed T cell specificity data into a heat map to visualize patterns of glucokinase-specific T cells in different individuals (Fig. 3d). From this analysis it was evident that some subjects had high frequencies for multiple epitopes (e.g., T1D #2 and T1D #5) whereas others had very few glucokinase-specific T cells (e.g., T1D #6). However, T1D #2, #5 and #6 all have detectable anti-glucokinase IgG (indicated at the bottom of Fig. 3d). We next asked whether the frequency

of glucokinase-reactive T cells might be correlated with characteristics such as disease duration, age at diagnosis biological sex, or levels of glucokinase specific antibodies. Considering both T1D patients and controls, we observed a significant positive correlation between the combined frequency of glucokinase-reactive T cells and levels of anti-glucokinase antibodies (Fig. 3e). No other associations reached significance.

The effect of citrullination on the biological function of glucokinase in pancreatic beta cells.

Pro-inflammatory cytokines are known to attenuate glucose stimulated insulin secretion (GSIS), mediated by glucokinase, as studied elsewhere [29, 30, 31]. We utilized a subclonal cell line from the parenteral INS-1 cells, INS-1E, to examine GSIS and how citrullination may alter the glucose sensing/insulin secreting metabolic pathway. We utilized YW3-56, a PAD2/PAD4 inhibitor, in studies of GSIS in INS-1E cells as a means of blocking protein citrullination. First, we confirmed by immunoblot detection of citrulline that IFNγ +IL-1β cytokine-induced citrullination levels were reduced in the presence of YW3-56 in INS-1E cells (Fig. 4a). As shown in the left panels of Fig. 4b, INS-1E cells secrete insulin in response to glucose in a dose-dependent manner (2.5, 5 and 16.7mM of D-(+)-glucose, white bar), while IFNγ +IL-1β cytokines diminished insulin secretion upon glucose stimulation (black bars). As expected, YW3-56 alone did not affect citrullination levels or GSIS in INS-1E cells (Fig. 4a & 4b, striped bar). Of note, YW3-56 can partially correct IFNγ +IL-1β suppressed GSIS at 16.7mM glucose when YW3-56 was cocultured with cytokines for 48 hours (grey bar in left panel of Fig. 4b). Interestingly, YW3-56 was able to correct IFNγ +IL-1β suppressed GSIS at 9mM glucose if INS-1E cells were cultured with YW3-56 throughout all the experiment setting including 48 hrs of cytokine treatment and 1 hr of glucose stimulation (data not shown). Using pyruvate instead

of glucose, beta cells will bypass glucokinase to stimulate insulin secretion [30]. Pyruvate stimulated insulin secretion was also found to decrease under IFNγ +IL-1β exposure (the right panel of Fig. 4b). Moreover, YW3-56 was also able to correct cytokine-mediated suppression of insulin secretion upon pyruvate stimulation. However, insulin secretion upon to depolarization with KCL was not affected by cytokines in the presence or absence of YW3-56 (the middle panel of Fig. 4b). *In toto*, our data suggest that IFNγ +IL-1β-triggered citrullination affects not only glycolysis (mediated by glucokinase) but also downstream metabolism from glycolysis in the insulin biosynthesis pathway. However, there appears to be no effect of citrullination on the depolarization step of insulin secretion in beta cells.

Recombinant human pancreatic glucokinase (rhGK) was used to map potential citrullination residues and ask if citrullination alters glucokinase catalytic activity. Full length of recombinant human pancreatic GK (rhGK) was incubated with PAD in the presence of Ca^{++}. Citrullinated rhGK migrates slightly slower on SDS-PAGE due to the loss of positive charge as shown in the left panel of Fig. 5a. Citrullination of GK was also confirmed by immunoblot (the right panel of Fig. 5a). By using mass spectrometry, there were 16 citrullination modification residues, found in PAD-treated rhGK (Fig. 5b). Thus, 50% of Arg residues (16 Arg out of total 32 Arg residues) were available to be citrullinated *in vitro* by PAD. One representative mass spectra demonstrated the citrullination sites are at Arg 428 and Arg 429 in PAD-treated rhGK peptides (a.a. 423-447) (supplementary Fig. 6a). As shown in Fig. 5c, citrullination of rhGK by PAD *in vitro* was found to reduce the catalytic activity of the enzyme by 20%. Next, we subjected the native rhGK and PAD-treated rhGK to steady-state kinetic analyses at 37°C with various concentration of substrate (glucose). PAD-treated rhGK demonstrated similar Vmax compared to native rhGK (119.9±7.7 μmol/mg/min of PAD-treated rhGK versus 115.1±10.5 μmol/mg/min

of native rhGK). However, the Km of PAD-treated rhGK was two-fold increased (16.2±2.3 mM) compared to native rhGK (8.48±2.1 mM) (Fig. 5d). These data reveal that glucokinase is a substrate of PAD and suggests citrullination can modulate its glucose threshold for insulin secretion in beta cells, mediated by reduced substrate binding affinity of glucokinase enzyme.

DISCUSSION

In the current study, our results reveal that citrullination alters the enzyme kinetics of glucokinase and reduces glucose stimulated insulin secretion (GSIS), the major biological function of pancreatic beta cells. We also demonstrate immune recognition of glucokinase in subjects with T1D, in that both antibodies against and autoreactive T cells that recognize glucokinase epitopes are present in the periphery.

The role of protein citrullination by PAD2/PAD4 in promoting loss of self-tolerance is well studied in RA. This represents a potentially effective therapeutic axis, in that several potent PAD4 specific inhibitors have been developed and were shown to disrupt mouse and human NET formation (NETosis) [22, 32, 33, 34] leading to improved cancer prognosis. NETosis has also been shown to be a major source of autoantigens in RA [33, 35] and its activity is also believed to form neo-epitopes in other autoimmune disease settings [16, 26, 36]. For the first time, we show that one PAD2/PAD4 inhibitor, YW3-56, can protect from inflammation-induced citrullination and partially restore insulin secretion in beta cells upon stimulation with glucose or pyruvate. Besides YW3-56, a specific PAD2 inhibitor, CAY10723, was also found to be able to restore cytokine-suppressed insulin secretion in INS-1E cells (data not shown). However, neither YW3-56 nor CAY10723 can completely restore cytokine-suppressed insulin secretion response to glucose or pyruvate. These observations suggest that inflammation-induced citrullination may not be the only mechanism for defective insulin biosynthesis in T1D.

As mentioned above, ATP-dependent glucokinase converts glucose to glucose-6-phosphate, the critical step in glucose metabolism. Alternative splicing of the glucokinase gene results in three tissue-specific isoforms, isoform 1 (pancreas) and isoforms 2 and 3 (liver). The only difference among three glucokinase isoforms is in the amino acid sequence of exon 1in the first

fifteen amino acids of human pancreatic glucokinase [37]. Unlike other hexokinases, glucokinase is not regulated by feedback inhibition by glucose-6-phosphate. Therefore, glucokinase can constitutively trigger insulin secretion in pancreatic β-cells under high glucose conditions. To date, few studies demonstrate any role of PTMs in altering glucokinase activity. Polyubiquitination of human glucokinase, both pancreatic isoform 1 and hepatic isoform 2 increases catalytic activity up to 1.4 fold [38]. SUMOylation (small ubiquitin-like modifiers) of glucokinase was found in MIN6 and INS-1 cells and results in increased pancreatic glucokinase stability and activity [39]. In the current study, our data suggest that citrullination impairs the major function of glucokinase in pancreatic beta cells, glucose sensor function, due to the suppression of substrate binding affinity of recombinant human pancreatic glucokinase (Fig. 5d).

Pancreatic beta cell-specific glucokinase knockout mice die within the first week of birth of severe hyperglycemia [40]. Besides NOD mice, the streptozotocin (STZ)-induced model of murine diabetes also resembles human T1D, recapitulating the phenomena of insulitis and insulin deficiency. Relevant to this study, STZ-induced diabetic mice exhibit decreased glucokinase expression with hyperglycemia [41]. PKM2 (one of four pyruvate kinase isozyme L, R, M1 and M2) activation protects against diabetes by increasing glucose metabolic flux and inducing mitochondria biogenesis [42]. Of note, the catalytic activity of PK is increased 2 to 3-fold after *in vitro* citrullination by PAD [43]. Our pilot studies identified citrullinated- and acetylated-PKM2 in IFN-γ and TNF-α-treated human islets but no such PTMs found in PKM2 from untreated control islets (data not shown). Collectively, our data suggest that citrullinated GK and perhaps other pathway proteins contributes to the defects of insulin secretion in beta cells.

In the current study, we found that the total citrullination levels were higher in 16 week old NOD inflamed pancreas compared to age-matched B6 pancreas. We found that both anti-GK

and anti-citrullinated GK IgG are significantly higher in NOD serum compared to age-matched B10.BR serum even before the diabetic onset, as early as 4-6 weeks of age. Similarly,, both anti-GK and anti-citrullinated GK IgG titers were significantly higher in patients with T1D compared to healthy subjects. Interestingly, both diagnostic anti-insulin and anti-ZnT8 antibodies correlated with anti-citrullinated GK in patients with T1D, raising the possibility of linked development. However, the broad disease duration (0.1-55 years) in our T1D serum samples limits our ability to determine whether anti-GK and/or anti-citrullinated GK could serve as a novel diagnostic antibody for T1D (Fig. 2c).

The loss of immune tolerance to PTMs within the stressed beta cells triggers an autoreactive T cell response and contributes to the destruction of insulin-producing beta cells in autoimmune diabetes. Emerging data demonstrate that autoreactive T cells against variety of PTMs-neoepitopes are found in patients with T1D including oxidation, deamidation, phosphorylation and citrullination [14]. For example, CD4 T cells from patients with T1D were identified to specifically recognize the oxidized insulin neoepitopes, near disulfide bond region in A chain, in the context of HLA-DR4 [44]. Previous studies demonstrated that the citrullination and transglutamination can enhance GAD65 peptide binding to HLA-DRB1*04:01 (DR0401) [26]. To date, GAD65, GRP78, islet-specific glucose 6 phosphatase catalytic subunit-related protein (IGRP) and islet amyloid polypeptide (IAPP) are identified as the citrullinated-neoepitopes recognized by autoreactive T cells in the development of T1D [7]. Herein, we investigated the relevance of T cell responses to glucokinase in human disease by identifying citrullinated and unmodified peptides that are bound and presented by DR0401, a part of the high-risk T1D-associated DR4/DQ8 haplotype [25], and recognized by human $CD4^+$ T cells. We then utilized the corresponding HLA class II tetramers to determine whether T cells that recognize glucokinase

are present within the peripheral blood of subjects with T1D. We identified a total of five immunogenic DR0401-restricted GK epitopes, one of which was citrullinated at Arg^{358} residue of GK. Notably, among the various GK epitopes identified through our study, the citrullinated GK 436 epitope emerged as the specificity with the highest median frequency and that best differentiated controls and subjects with T1D. Consistent with this data, we observed that Arg^{358} residue of GK is highly susceptible to citrullination in PAD-treated recombinant human pancreatic GK protein (Fig. 5b). Moreover, Arg^{358} residue of GK was identified to be citrullinated in cytokine treated- but not in untreated INS-1E beta cells (Supplementary Fig. 6 b & c).

Neoepitopes derived from citrullination modification of islet proteins, citrullinated GK and/or other unknown glucose-insulin metabolic proteins, breaks immune tolerance to trigger T and B cell autoimmunity. Perhaps more importantly, citrullination of GK impairs islet responses to glucose and overall glucose homeostasis. The pathway of cytokine stress and citrullination is an amplifying feedback loop of T1D pathology that includes both autoimmunity and altered beta cell metabolism. The pathway can potentially be interrupted by therapeutic manipulation of the tissue microenvironment preventing the development of citrullination (PAD inhibitors) or by the inhibition of proinflammatory cytokines in the pancreas.

METHODS

Mice. Female NOD/ShiLt, C57BL/6, and B10.BR mice were purchased at 3 wks of age from Jackson Laboratories (Bar Harbor, Maine). All mice were housed in microisolator cages with free access to food and water and maintained at the Yale Animal Resource Center at Yale University. All animal studies were performed in accordance with the guidelines of the Yale University Institutional Animal Care and Use Committee. Glucose levels were measured in blood withdrawn from the retroorbital sinus of anesthetized mice using Lite glucometer and test strips (Abbott Laboratories, Abbott Park, IL, USA). Mice with blood glucose values greater than 250 mg/dL were considered diabetic. Serial serum samples were acquired from NOD and age matched control animals. Pancreas and liver tissue extract were prepared in RIPA buffer containing a mixture of protease inhibitors (Complete protease inhibitor, Roche Diagnostics).

Protein citrullination detection. Presence of citrullinated protein was detected by using anti-citrulline (ab6464; Abcam) for immunohistochemistry as described elsewhere [45], by using anti-peptidyl-citrulline, clone F95 (Millipore) for flow cytometry and confocal microscopy and by using anti-modified citrulline detection kit (clone C4; Millipore) for immunoblot according to manufacturer's protocol.

For flow cytometry, beta cells were dissociated into single-cell suspension by trypsin (Millipore) and fixed by 95% methanol and 4% paraformaldehyde for 30 min on ice. Cells were stained with anti-peptidyl-citrulline, clone F95 (Millipore), and anti-mouse Alexa Fluor 488 (Life Technology) for intracellular citrullination level and/or with anti-glucokinase (Proteintech) and anti-rabbit Alexa Fluor 647 (Life Technology) for glucokinase expression in staining buffer

(PBS containing 1% BSA and 0.1% Tween-20). Stained cells were analyzed by FACSCalibur (BD Biosciences) with FlowJo software (Tree Star).

For confocal microscopy, beta cells were fixed by 95% methanol for 30 min, washed twice with PBS and permeabilized with 0.3% Triton X-100 for 2 h. Then the cells were stained with anti-peptidyl-citrulline, clone F95 (Millipore). Cells were then observed on a Leica SP5 II laser scanning confocal microscope.

Beta cell cultures and insulin secretion assay. The INS-1 rat insulinoma cells were cultured at 37°C in RPMI-1640 (Thermal Fisher Scientific) containing 11.2 mM glucose and 2 mM L-glutamine and supplemented with 10% fetal bovine serum (FBS), 50 μM β-mercaptoethanol, 100 units/ml penicillin, and 100 μg/ml streptomycin. For cytokine stress, the INS-1 cells were treated with recombinant mouse IFNγ (1000 units/mL; R&D Systems) and recombinant human IL-1β (50 units/mL; R&D Systems) and harvest for citrullination detection as described above.

For insulin secretion assay, the INS-1E cells, a gift from Prof. Wollheim (CMU, Geneva, Switzerland) [46], were seeded on 6 well plate and cultured with recombinant mouse IFNγ (100 units/mL; R&D Systems) and recombinant human IL-1β (5 units/mL; R&D Systems) in the presence or absence of PAD2/PAD4 inhibitor (5 μM YW3-56; Cayman) for 48 hrs. Cells were washed and starved for 1 hr in low-glucose KREBS buffer (138mM NaCl, 4.7mM KCl, 1mM $CaCl_2$, 1.18mM KH_2PO4, 1.18mM MgSO4, 5mM $NaHCO_3$, 25mM Hepes (pH7.4), 0.1% BSA and 2.5mM glucose). Assay buffer was then replaced with KREBS buffer containing either varying glucose concentration (2.5, 5, 9 and 16.7mM), 10mM sodium pyruvate or 30mM KCl. After another 1 hr incubation, supernatants were collected and assayed for insulin by using Rat

High Range Insulin ELISA kit (ALPCP) according to manufacturer's protocol. All experiments were performed using INS-1E cells between the 61st and 65th passage.

***In vitro* citrullination and identification of citrullination sites by LC-MS/MS.** For *in vitro* citrullination, 0.1U of rabbit peptidylarginine deiminase (PADI2; Sigma-Aldrich) were added to 50 µg of recombinant human pancreatic glucokinase (rhGK; LS-G3456, LSBio) in reaction buffer (0.1M Tris-HCl, 10mM CaCl2 and 5mM DTT) at 37°C for 2.5 hrs and kept at -80°C in multiple aliquots to avoid freeze and thaw until used. Minimum 6 µg of rhGK and PAD-treated-rhGK were reduced, alkylated and tryptic digested for LS-MS/MS analysis. Data were collected on a QE-Plus mass spectrometer coupled to a NanoACQUITY UPLC (Waters Inc.). A Waters Symmetry® C18 180 µm × 20 mm trap column and a 1.7-µm, 75 µm × 250 mm nanoACQUITY UPLC column (35°C) was utilized for the separation. Collected LC MS/MS data were processed using Proteome Discoverer Software (v. 2.2, Thermo Fisher Scientific) and searched were carried out in MASCOT Search Engine (Matrix Science) using the below parameters; oxidation (M), deamidated (N/Q) and citrullination (R) as the variable modifications and carbamidomethylation (C) as a fixed modification. Mascot results were loaded into Scaffold Q+S 4.11.0 and then Scaffold PTM 3.3.0 was used to re-analyzes MS/MS spectra identified as modified peptides and calculates Ascore values and site localization probabilities to assess the level of confidence in each PTM localization. Scaffold PTM then combines localization probabilities for all peptides containing each identified PTM site to obtain the best estimated probability that a PTM is present at that particular site.

For identification of citrullination residues in intracellular glucokinase in INS-1E cells, cells were scraped from cytokine treated and control cells and centrifuged for 5 minutes at 1,300 g. The

cell pellet was lysed in 400 µL 1% CHAPS buffer (1% CHAPS, 100 mM KCl, 150 mM NaCl, 50 mM Tris-HCl pH 7.5 and a mixture of protease inhibitors (Complete protease inhibitor, Roche Diagnostics)) and kept on ice for 30 minutes with occasional tapping. Cell debris was removed by centrifuging 10 minutes at 4°C at 13,000 RPM. Proteins smaller than 30 kDa were removed by passing the protein lysate through an Amicon Ultra – 15 Centrifugal Filter (Millipore). One mg of cell lysate in 500 µL lysis buffer was pre-cleared by adding 10 µL of protein A/G PLUS-agarose beads (Santa Cruz) and incubating for 1 hour at 4°C on a rotator. Cell lysate was centrifuged for 4 minutes at 4°C at 2,000 RPM and the supernatant was incubated overnight at 4°C on a rotator with 5 µg of anti-glucokinase antibody (Proteintech). Thirty µL of protein A/G PLUS-agarose beads were washed with 500 µL wash buffer (500 mM NaCl, 50 mM Tris-HCl pH 7.5 and 0.05% (v/v) Tween-20) and with 200 µL 1% CHAPS buffer. The cell lysate was added to the beads and incubated overnight at 4°C on a rotator. The samples were washed 4 times with 250 µL 1% CHAPS buffer and 3 times with pre-urea buffer (50 mM Tris pH 8.5, 1 mM EGTA and 75 mM KCl). Then 75 µL urea elution buffer (7 M urea, 20 mM Tris pH 7.5 and 100 mM NaCl) was added and the samples were rotated for 30 minutes at room temperature. The beads were pelleted and the supernatant was kept aside. This process was repeated twice to ensure that all the captured proteins are released from the beads. Eluted proteins were protein precipitated using the Wessel-Flügge method [47]. The protein precipitates were dissolved in urea buffer (7M urea in 1M Tris-HCl pH 8). Samples were prepared for analysis on LC-MS/MS as above and run on a QExactive Orbitrap (Thermo Fisher Scientific). Peptides were identified by MASCOT (Matrix Science) using SwissProt (Homo sapiens, 169779 entries) as a database via Proteome Discoverer 2.2, incorporating Percolator for peptide validation. Same parameters of variable modifications and fixed modification were set as mentioned above. Two missed cleavages were allowed, peptide

tolerance was set at 5 ppm and MS/MS tolerance at 20 mmu. The MS/MS spectra were carefully checked manually for the presence of citrullinated residues.

ELISA and immunoblot assay. Immunoreactivity of human and mouse serum to rhGK and PAD-treated-rhGK was performed by ELISA. Briefly, 0.5 µg of rhGK or PAD-treated-rhGK in 0.05 M carbonate-bicarbonate buffer (pH = 9.6; Sigma) was coated onto ELISA plates (Thermo Fisher Scientific) overnight at 4°C and blocked with 1%BSA in PBST containing 1% Tween-20. Sera were diluted as 1:100 in diluting buffer (0.03% BSA in PBST) and incubated 2 h at room temperature. Species-specific goat anti-IgG alkaline phosphatase was used as a secondary reagent (Southern Biotech). Color was developed via the addition of pNPP substrate (Sigma) and absorbance was read at 405nm (Synergy HT Multi-Mode Reader, BioTek Instruments). Individual signals were normalized to no-antigen control wells. Rabbit polyclonal antibody against glucokinase (Proteintech) served as positive control in ELISA. All readings were normalized to non-specific serum binding to no-antigen control wells. Autoantibodies against to rhGK or PAD-treated-rhGK was designating as positive with an OD > 2 standard deviation (SD) above B10.BR serum or human healthy serum.

For immunoblotting, 1 µg of rhGK or PAD-treated-rhGK was subjected to electrophoresis, blotted onto a nitrocellulose membrane, and probed with serum (1:100) from B10.BR or NOD mice and incubated with the alkaline phosphatase-conjugated anti-mouse IgG, then visualized by NBT/BCIP substrate (Thermo Fisher Scientific).

Catalytic activity of recombinant human pancreatic glucokinase. After *in vitro* citrullination by PAD as described above, recombinant human pancreatic glucokinase (rhGK; LS-G5486,

LSBio) was put on the ice to stop the reaction for 5 min. Then glucokinase activity was measured spectrophotometrically (A340nm) at 37°C by a glucose 6-phosphate dehydrogenase (G6PDH) coupled assay as described previously [48]. In brief, 1µg rhGK or PAD-treated rhGK was assayed in a reaction buffer containing 25mM Hepes (pH7.3), 2mM MgCl2, 1mM DTT, 0.5mM NADP, 2mM ATP, 0.01%BSA, 20U/ml G6PDH and 25mM D-(+)-glucose. Relative specific activity of glucokinase was calculated from linear regression of the change in A340nm. To determine the steady-state kinetic properties of both rhGK and PAD-treated rhGK, varying concentrations of D-(+)-glucose (0-50mM) were used. Vmax and Km were calculated by Michaelis-Menten equation using GraphPad Prism Software.

Human samples. Two sets of human samples were used in this study. For anti-glucokinase and anti-citrullinated glucokinase antibodies by ELISA, human serum samples were collected from subjects with longstanding T1D (n=55). IRB approval for the study was sought and received from the Benaroya Research Institute IRB. Samples were assayed in a blinded fashion for ELISA as described above. The presence or absence of autoantibodies against to GAD65, IA2, ZnT8 and insulin were determined by Barbara Davis Center Autoantibody/HLA Service Center using standardized radioimmunoassay.

For HLA tetramer staining assays, peripheral blood and serum were collected from 10 individuals with T1D and 10 healthy controls with DRB1*04:01 haplotypes after obtaining written consent under a study approved by the Institutional Review Board at the Benaroya Research Institute. Subject attributes are summarized in Supplemental Tables 3 and 4.

Peptide prediction. The probability that citrullinated and unmodified glucokinase peptides would be bound and presented by DR0401 was evaluated based on a previously published prediction matrix [13, 26]. Briefly, coefficients corresponding to each anchor residue for all possible core 9-mers within the protein were multiplied, yielding a predicted relative binding affinity score. Sequences were chosen to include at least 2 flanking residues on each side of the predicted minimal 9-mer motif.

Peptide binding measurements. Peptides with predicted binding to DR0401 (Supplemental Table 3) were synthesized (Sigma) and their binding to DR0401 was assessed through a competition assay, as previously described [49]. Briefly, increasing concentrations of each citrullinated glucokinase peptide were incubated in competition with a biotinylated reference influenza hemagglutinin peptide ($HA_{306-318}$) at 0.02 μM in wells coated with DR0401 protein. After washing, residual biotin-$HA_{306-318}$ was detected using europium-conjugated streptavidin (Perkin Elmer) and quantified using a Victor2D time resolved fluorometer (Perkin Elmer). Curves were simulated using Prism software (Version 5.03, GraphPad Software Inc.) and IC_{50} values calculated as the concentration needed to displace 50% of the reference peptide.

HLA Class II protein and Tetramer reagents. DR0401 protein was purified from insect cell cultures as previously described [50, 51]. Monomers were loaded with 0.2 mg/ml peptide at 37°C for 72 h in the presence of 0.2 mg/ml n-Dodecyl-β-maltoside and 1 mM Pefabloc (Sigma–Aldrich). Peptide-loaded monomers were conjugated into tetramers using R-PE streptavidin (Invitrogen), PE-Cy5 streptavidin (BD), or PE-CF594 streptavidin at a molar ratio of 8:1.

***In vitro* tetramer assays and T cell clone isolation.** Peripheral blood mononuclear cells (PBMCs) were isolated by Ficoll underlay, resuspended in T cell media (RPMI, 10% pooled human serum, 1% Penicillin-Streptomycin, 1% L-glutamine) at 4×10^6 cells/mL, and stimulated with peptides (20 µg/mL total) in 48-well plates for 14 days, adding medium and IL-2 starting on day 7. Cells were stained with individual tetramers for 75 minutes at 37°C, followed by CD4 BV650 (BD Biosciences), CD3 APC (eBioscience), and CD25 FITC (BioLegend) for 15 minutes at 4°C, run on a FACSCalibur (BD), and analyzed using FlowJo (Treestar Inc). Clones were isolated by sorting single tetramer-positive CD4+ T cells using a FACS Aria (BD) and expanded in 96-well plates in the presence of 1×10^5 irradiated PBMC, 2 µg/mL phytohaemagglutinin (Remel Inc.), adding media and IL-2 starting on day 10.

T cell clone maintenance and characterization. Clones specific for citrullinated Glucokinase peptides were maintained in supplemented RPMI and re-stimulated using PHA (2 µg/mL; Remel) every two weeks. Specificity was confirmed by re-staining expanded clones with tetramer.

Ex vivo tetramer analysis. Analysis of T cell frequency was accomplished using our previously published approach [28]. Briefly, $40\text{-}60\times10^6$ PBMCs were re-suspended in a total of 400-600 µL of media, divided into two independent tubes of 20×10^6 cells (200 µL) each, incubated with 50 nM dasatinib for 10 minutes at 37°C, and stained with 20 µg/mL of PE-labeled, PE-CF594-lableled, or PE-Cy5-labled tetramers at room temperature for 120 minutes (three tetramers per tube, a total of 6 glucokinase tetramers). Cells were washed, incubated with PE-magnetic beads (Miltenyi) for 20 minutes at 4°C and magnetically enriched, retaining 1% of

the cells as a non-enriched sample. Enriched (bound) and non-enriched (pre-column) samples were stained with CD4 V500, CD14 PerCP-Cy5.5, CD19 PerCP-Cy5.5 (eBioscience), CD45RA AF700 (BD), CXCR3 FITC, CCR6 BV421, and CCR4 BV605 (BioLegend) for 15 minutes at 4°C. After washing, cells were labeled with ViaProbe (BD Biosciences) and analyzed on a FACSCanto (BD Biosciences), gating on $CD4^{+}CD14^{-}CD19^{-}ViaProbe^{-}$ cells and plotting tetramer versus CD45RA. Frequencies were calculated as previously described [28].

Statistical analysis. Statistics were performed using a Student's unpaired two-tailed *t* test unless indicated. A value of $p < 0.05$ was regarded as significant.

Acknowledgements

We thank members of the Mamula laboratory, Emily Schroeder and Tyler Masters for excellent technical assistant for this study. This research was supported by the Juvenile Diabetes Research Foundation (Innovative Grant to M.J.M. and 2-SRA-2018-551-S-B to E.A.J.), and National Institutes of Health (DK104205-01 to K.H. and M.J.M.).

Author contributions

M.L.Y. designed and performed the experiments, analyzed the data, and wrote the manuscript. S.H. and R.G. performed the experiments and analyzed data; T.T.L. and J. K. performed the proteomic PTM analysis and edited the manuscript. C.S. and C.J.G. were responsible for subject selection and clinical characterization and edited the manuscript. E.A.J. and L.O. designed the experiments, summarized data and co-wrote the manuscript. A. P., R.G.K., and K.C.L. provided

helpful advice and edited the manuscript. M.J.M. directed the project, edited the manuscript and was responsible for coordination and strategy.

Competing interests

The authors declare no competing financial interests.

References: References

1. Sternisha SM, Miller BG. Molecular and cellular regulation of human glucokinase. *Arch Biochem Biophys* 2019, **663:** 199-213.

2. Matschinsky FM. Assessing the potential of glucokinase activators in diabetes therapy. *Nat Rev Drug Discov* 2009, **8**(5)**:** 399-416.

3. Hattersley AT, Turner RC, Permutt MA, Patel P, Tanizawa Y, Chiu KC*, et al.* Linkage of type 2 diabetes to the glucokinase gene. *Lancet* 1992, **339**(8805)**:** 1307-1310.

4. Froguel P, Zouali H, Vionnet N, Velho G, Vaxillaire M, Sun F*, et al.* Familial hyperglycemia due to mutations in glucokinase. Definition of a subtype of diabetes mellitus. *N Engl J Med* 1993, **328**(10)**:** 697-702.

5. Nakamura A, Terauchi Y. Present status of clinical deployment of glucokinase activators. *J Diabetes Investig* 2015, **6**(2)**:** 124-132.

6. Zhu D, Gan S, Liu Y, Ma J, Dong X, Song W*, et al.* Dorzagliatin monotherapy in Chinese patients with type 2 diabetes: a dose-ranging, randomised, double-blind, placebo-controlled, phase 2 study. *Lancet Diabetes Endocrinol* 2018, **6**(8)**:** 627-636.

7. Yang ML, Doyle HA, Clarke SG, Herold KC, Mamula MJ. Oxidative Modifications in Tissue Pathology and Autoimmune Disease. *Antioxid Redox Signal* 2018, **29**(14)**:** 1415-1431.

8. Makrygiannakis D, af Klint E, Lundberg IE, Lofberg R, Ulfgren AK, Klareskog L*, et al.* Citrullination is an inflammation-dependent process. *Ann Rheum Dis* 2006, **65**(9)**:** 1219-1222.

9. Zendman AJ, Vossenaar ER, van Venrooij WJ. Autoantibodies to citrullinated (poly)peptides: a key diagnostic and prognostic marker for rheumatoid arthritis. *Autoimmunity* 2004, **37**(4)**:** 295-299.

10. Feitsma AL, van der Voort EI, Franken KL, el Bannoudi H, Elferink BG, Drijfhout JW*, et al.* Identification of citrullinated vimentin peptides as T cell epitopes in HLA-DR4-positive patients with rheumatoid arthritis. *Arthritis Rheum* 2010, **62**(1)**:** 117-125.

11. Snir O, Rieck M, Gebe JA, Yue BB, Rawlings CA, Nepom G*, et al.* Identification and functional characterization of T cells reactive to citrullinated vimentin in HLA-DRB1*0401-positive humanized mice and rheumatoid arthritis patients. *Arthritis Rheum* 2011, **63**(10)**:** 2873-2883.

12. Chemin K, Pollastro S, James E, Ge C, Albrecht I, Herrath J*, et al.* A Novel HLA-DRB1*10:01-Restricted T Cell Epitope From Citrullinated Type II Collagen Relevant to Rheumatoid Arthritis. *Arthritis Rheumatol* 2016, **68**(5)**:** 1124-1135.

13. James EA, Rieck M, Pieper J, Gebe JA, Yue BB, Tatum M*, et al.* Citrulline-specific Th1 cells are increased in rheumatoid arthritis and their frequency is influenced by disease duration and therapy. *Arthritis Rheumatol* 2014, **66**(7)**:** 1712-1722.

14. McGinty JW, Marre ML, Bajzik V, Piganelli JD, James EA. T cell epitopes and post-translationally modified epitopes in type 1 diabetes. *Curr Diab Rep* 2015, **15**(11)**:** 90.

15. Rondas D, Crevecoeur I, D'Hertog W, Ferreira GB, Staes A, Garg AD*, et al.* Citrullinated glucose-regulated protein 78 is an autoantigen in type 1 diabetes. *Diabetes* 2015, **64**(2)**:** 573-586.

16. Buitinga M, Callebaut A, Marques Camara Sodre F, Crevecoeur I, Blahnik-Fagan G, Yang ML*, et al.* Inflammation-Induced Citrullinated Glucose-Regulated Protein 78 Elicits Immune Responses in Human Type 1 Diabetes. *Diabetes* 2018, **67**(11)**:** 2337-2348.

17. Witalison EE, Thompson PR, Hofseth LJ. Protein Arginine Deiminases and Associated Citrullination: Physiological Functions and Diseases Associated with Dysregulation. *Curr Drug Targets* 2015, **16**(7)**:** 700-710.

18. Klareskog L, Widhe M, Hermansson M, Ronnelid J. Antibodies to citrullinated proteins in arthritis: pathology and promise. *Curr Opin Rheumatol* 2008, **20**(3)**:** 300-305.

19. Vossenaar ER, Zendman AJ, van Venrooij WJ, Pruijn GJ. PAD, a growing family of citrullinating enzymes: genes, features and involvement in disease. *Bioessays* 2003, **25**(11)**:** 1106-1118.

20. Wang S, Wang Y. Peptidylarginine deiminases in citrullination, gene regulation, health and pathogenesis. *Biochim Biophys Acta* 2013, **1829**(10)**:** 1126-1135.

21. Damgaard D, Senolt L, Nielsen CH. Increased levels of peptidylarginine deiminase 2 in synovial fluid from anti-CCP-positive rheumatoid arthritis patients: Association with disease activity and inflammatory markers. *Rheumatology (Oxford)* 2016, **55**(5)**:** 918-927.

22. Crevecoeur I, Gudmundsdottir V, Vig S, Marques Camara Sodre F, D'Hertog W, Fierro AC*, et al.* Early differences in islets from prediabetic NOD mice: combined microarray and proteomic analysis. *Diabetologia* 2017, **60**(3)**:** 475-489.

23. Matschinsky FM. Glucokinase as glucose sensor and metabolic signal generator in pancreatic beta-cells and hepatocytes. *Diabetes* 1990, **39**(6)**:** 647-652.

24. Iynedjian PB, Mobius G, Seitz HJ, Wollheim CB, Renold AE. Tissue-specific expression of glucokinase: identification of the gene product in liver and pancreatic islets. *Proc Natl Acad Sci U S A* 1986, **83**(7)**:** 1998-2001.

25. Erlich H, Valdes AM, Noble J, Carlson JA, Varney M, Concannon P*, et al.* HLA DR-DQ haplotypes and genotypes and type 1 diabetes risk: analysis of the type 1 diabetes genetics consortium families. *Diabetes* 2008, **57**(4)**:** 1084-1092.

26. McGinty JW, Chow IT, Greenbaum C, Odegard J, Kwok WW, James EA. Recognition of posttranslationally modified GAD65 epitopes in subjects with type 1 diabetes. *Diabetes* 2014, **63**(9)**:** 3033-3040.

27. Rims C, Uchtenhagen H, Kaplan MJ, Carmona-Rivera C, Carlucci P, Mikecz K*, et al.* Citrullinated Aggrecan Epitopes as Targets of Autoreactive CD4+ T Cells in Patients With Rheumatoid Arthritis. *Arthritis Rheumatol* 2019, **71**(4)**:** 518-528.

28. Kwok WW, Roti M, Delong JH, Tan V, Wambre E, James EA*, et al.* Direct ex vivo analysis of allergen-specific CD4+ T cells. *J Allergy Clin Immunol* 2010, **125**(6)**:** 1407-1409 e1401.

29. Burke SJ, Stadler K, Lu D, Gleason E, Han A, Donohoe DR*, et al.* IL-1beta reciprocally regulates chemokine and insulin secretion in pancreatic beta-cells via NF-kappaB. *Am J Physiol Endocrinol Metab* 2015, **309**(8)**:** E715-726.

30. Barlow J, Solomon TPJ, Affourtit C. Pro-inflammatory cytokines attenuate glucose-stimulated insulin secretion from INS-1E insulinoma cells by restricting mitochondrial pyruvate oxidation capacity - Novel mechanistic insight from real-time analysis of oxidative phosphorylation. *PLoS One* 2018, **13**(6)**:** e0199505.

31. Hostens K, Pavlovic D, Zambre Y, Ling Z, Van Schravendijk C, Eizirik DL*, et al.* Exposure of human islets to cytokines can result in disproportionately elevated proinsulin release. *J Clin Invest* 1999, **104**(1)**:** 67-72.

32. Tohme S, Yazdani HO, Al-Khafaji AB, Chidi AP, Loughran P, Mowen K*, et al.* Neutrophil Extracellular Traps Promote the Development and Progression of Liver Metastases after Surgical Stress. *Cancer Res* 2016, **76**(6)**:** 1367-1380.

33. Lewis HD, Liddle J, Coote JE, Atkinson SJ, Barker MD, Bax BD*, et al.* Inhibition of PAD4 activity is sufficient to disrupt mouse and human NET formation. *Nat Chem Biol* 2015, **11**(3)**:** 189-191.

34. Li M, Lin C, Deng H, Strnad J, Bernabei L, Vogl DT*, et al.* A Novel Peptidylarginine Deiminase 4 (PAD4) Inhibitor BMS-P5 Blocks Formation of Neutrophil Extracellular Traps and Delays Progression of Multiple Myeloma. *Mol Cancer Ther* 2020, **19**(7)**:** 1530-1538.

35. Corsiero E, Pratesi F, Prediletto E, Bombardieri M, Migliorini P. NETosis as Source of Autoantigens in Rheumatoid Arthritis. *Front Immunol* 2016, **7:** 485.

36. Yang L, Tan D, Piao H. Myelin Basic Protein Citrullination in Multiple Sclerosis: A Potential Therapeutic Target for the Pathology. *Neurochem Res* 2016, **41**(8)**:** 1845-1856.

37. Tanizawa Y, Matsutani A, Chiu KC, Permutt MA. Human glucokinase gene: isolation, structural characterization, and identification of a microsatellite repeat polymorphism. *Mol Endocrinol* 1992, **6**(7)**:** 1070-1081.

38. Bjorkhaug L, Molnes J, Sovik O, Njolstad PR, Flatmark T. Allosteric activation of human glucokinase by free polyubiquitin chains and its ubiquitin-dependent cotranslational proteasomal degradation. *J Biol Chem* 2007, **282**(31)**:** 22757-22764.

39. Aukrust I, Bjorkhaug L, Negahdar M, Molnes J, Johansson BB, Muller Y*, et al.* SUMOylation of pancreatic glucokinase regulates its cellular stability and activity. *J Biol Chem* 2013, **288**(8)**:** 5951-5962.

40. Postic C, Shiota M, Niswender KD, Jetton TL, Chen Y, Moates JM*, et al.* Dual roles for glucokinase in glucose homeostasis as determined by liver and pancreatic beta cell-specific gene knock-outs using Cre recombinase. *J Biol Chem* 1999, **274**(1)**:** 305-315.

41. Lu G, Teng X, Zheng Z, Zhang R, Peng L, Zheng F*, et al.* Overexpression of a glucokinase point mutant in the treatment of diabetes mellitus. *Gene Ther* 2016, **23**(4)**:** 323-329.

42. Qi W, Keenan HA, Li Q, Ishikado A, Kannt A, Sadowski T*, et al.* Pyruvate kinase M2 activation may protect against the progression of diabetic glomerular pathology and mitochondrial dysfunction. *Nat Med* 2017, **23**(6)**:** 753-762.

43. Tilvawala R, Nguyen SH, Maurais AJ, Nemmara VV, Nagar M, Salinger AJ*, et al.* The Rheumatoid Arthritis-Associated Citrullinome. *Cell Chem Biol* 2018, **25**(6)**:** 691-704 e696.

44. Mannering SI, Harrison LC, Williamson NA, Morris JS, Thearle DJ, Jensen KP*, et al.* The insulin A-chain epitope recognized by human T cells is posttranslationally modified. *J Exp Med* 2005, **202**(9)**:** 1191-1197.

45. Mohamed BM, Boyle NT, Schinwald A, Murer B, Ward R, Mahfoud OK*, et al.* Induction of protein citrullination and auto-antibodies production in murine exposed to nickel nanomaterials. *Sci Rep* 2018, **8**(1)**:** 679.

46. D'Hertog W, Overbergh L, Lage K, Ferreira GB, Maris M, Gysemans C*, et al.* Proteomics analysis of cytokine-induced dysfunction and death in insulin-producing INS-1E cells: new insights into the pathways involved. *Mol Cell Proteomics* 2007, **6**(12)**:** 2180-2199.

47. Wessel D, Flugge UI. A method for the quantitative recovery of protein in dilute solution in the presence of detergents and lipids. *Anal Biochem* 1984, **138**(1)**:** 141-143.

48. Molnes J, Bjorkhaug L, Sovik O, Njolstad PR, Flatmark T. Catalytic activation of human glucokinase by substrate binding: residue contacts involved in the binding of D-glucose to the super-open form and conformational transitions. *FEBS J* 2008, **275**(10)**:** 2467-2481.

49. Ettinger RA, Kwok WW. A peptide binding motif for HLA-DQA1*0102/DQB1*0602, the class II MHC molecule associated with dominant protection in insulin-dependent diabetes mellitus. *J Immunol* 1998, **160**(5)**:** 2365-2373.

50. Chow IT, Yang J, Gates TJ, James EA, Mai DT, Greenbaum C*, et al.* Assessment of CD4+ T cell responses to glutamic acid decarboxylase 65 using DQ8 tetramers reveals a pathogenic role of GAD65 121-140 and GAD65 250-266 in T1D development. *PloS one* 2014, **9**(11)**:** e112882.

51. Yang J, Chow IT, Sosinowski T, Torres-Chinn N, Greenbaum CJ, James EA*, et al.* Autoreactive T cells specific for insulin B:11-23 recognize a low-affinity peptide register in human subjects with autoimmune diabetes. *Proceedings of the National Academy of Sciences of the United States of America* 2014, **111**(41)**:** 14840-14845.

Figure Legends

Figure 1. The citrullination of glucokinase in NOD pancreas, but not in liver. a, Representative immunodetection of citrullinated proteins in NOD pancreas tissue sections at different ages (between 3.5 and 16 weeks of age). Brown staining demonstrates positive immunohistochemical reaction for citrulline by using anti-citrulline antibody. **b,** Representative H&E (left panel) and anti-CD3 (right panel) staining of pancreas from 16 weeks old NOD mice. **c-d,** Representative tissue extracted proteins, 50 μg per lane, from liver (L) or pancreas (P) of C57Bl/6 (B6) and NOD mice (16 weeks old) were separated on SDS-polyacrylamide gel electrophoresis (PAGE), and protein spots were stained by anti-modified citrulline detection kit (**c**) and anti-glucokinase (**d**). PAD-treated recombinant human glucokinase (PAD-rhGK) serves as the positive control for protein citrullination (**c**). **e,** The tissue extracted proteins from NOD

mice (16 weeks old) were immunoprecipitated using anti-glucokinase and immunoblotted with anti-peptidyl citrulline and anti-glucokinase as indicated.

Figure 2. The prevalence of autoantibodies against glucokinase and citrullinated glucokinase in both murine and human models of T1D. a, rhGK and PAD-rhGK (1µg per lane) were subjected to electrophoresis and followed by immunoblot with rabbit anti-GK as positive control (+) and sera from 16-week-old B10.BR and NOD mice, each lane indicates different mouse. **b-c**, The serum levels of anti-glucokinase and anti-citrullinated glucokinase from NOD mice and control mice (**b**) and from patients with T1D and healthy subjects (**c**) were measured by ELISA as described in Methods. The number of samples analyzed is indicated at the bottom of each group and the error bars indicated SD of mean. *, $p<0.05$; **, $p<0.005$.

Figure 3. Glucokinase specific $CD4^+$ T cells are more frequent in subjects with T1D and are correlated with antibody levels. a, Comparison of total glucokinase reactive $CD4^+$ T cell frequencies in the peripheral blood of 10 healthy controls and 10 subjects with T1D. The total frequencies of glucokinase-reactive T cells (GK 192, 199, 231, 266, 270, and 346 combined) were significantly higher ($p=0.0007$, Mann Whitney test) in subjects with T1D (black circles) than in HLA matched controls (white circles). **b**, Glucokinase specific $CD4^+$ T cells tended to be more naïve (CD45RA+CR7+) in healthy controls than in subjects with T1D had a significantly higher ($p=0.064$, Mann Whitney test). **c**, Individual frequencies were significantly higher in subjects with T1D (black circles) than in healthy controls (white circles) for GK 346 ($p=0.0004$, ANOVA followed by Sidak's multiple comparisons test). Individual frequencies trended toward being higher for GK 199 and GK 270 ($p=0.08$ and $p=0.09$ respectively) but did not reach

statistical significance. **d**, A heatmap analysis of individual glucokinase T cell frequencies in subjects with T1D, indicating patterns of reactivity that differed between subjects. In the heatmap each column represents one subject and each row reflects one glucokinase specificity, with each square color coded to indicate the observed T cell frequency in cells per million. The antibody readout is indicated at the bottom individually. **e**, There was a significant positive correlation between the combined frequency of glucokinase-reactive T cells and levels of anti-glucokinase antibodies (p=0.030, simple linear regression).

Figure 4. PAD inhibitor reduces overall citrulline modification and partially restore cytokine mediated defective insulin secretion in INS-1E beta cells. a, INS-1E cells were grown in fully supplementary DMEM or cultured with IFNγ (100U/ml) plus IL-1β (5U/ml) in the presence or absence of YW3-56 for 48 hrs. Then cell lysate were subjected to electrophoresis and followed by immunoblot with anti-modified citrulline. **b**, Similar with above, INS-1E cells were grown in fully supplementary DMEM (white and striped bar) or cultured with IFNγ plus IL-1β for 48 hrs (black and grey bar). Then the cells were stimulated with glucose, KCl or pyruvate for one hr in the absence (white and black bar) or presence of YW3-56 (grey and striped bar) followed by insulin measurement as described in Methods. Data are from one experiment representative of three independent experiments and the error bars indicated SD of mean. *, $p<0.05$.

Figure 5. Citrullination modifications in human pancreatic glucokinase. a, The citrullinated-rhGK was generated as described in Methods based on *in vitro* citrullination by PAD. The native and PAD treated-rhGK were subjected to electrophoresis and followed by

immunoblot with anti-glucokinase (α-GK) and anti-citrulline (α-citrulline). **b**, Sequence of human glucokinase demonstrated 16 arginines targeted by *in vitro* citrullination (shown as bold captical "R"). The six immunogenic peptides identified from tetramer staining assay are shown as underlined. *; Arg 358. **c**, The catalytic activity was measured spectrophotometrically at 25mM glucose on 1μg of rhGK and PAD treated-rhGK, respectively. The error bars indicated SD of mean. (n=3; *, p< 0.05,). **d**, The enzyme kinetics analysis of GK was measured with 7 dilutions of glucose (0-50mM). Then the data were analyzed by Michaelis-Menten equation using GraphPad Prism Software.

Table 1. Sequences and binding affinities for antigenic glucokinase peptides

Peptide	Amino acid sequence[a]	IC50[b] (μM)
GK 192	RGD**FEMDVVAMV**NDT	0.35
GK 199	VVA**MVNDTVATM**ISCY	2.5
GK 266	LDE**FL**<u>**LEYDRLV**</u>DES	5.6
GK 270	LLE**YDR**<u>**LVDESS**</u>ANP	2.0
GK 346	KQI<u>YNI</u>**LSTLGL[Cit]PS**	0.47

[a] The predicted minimal epitope is bolded in each sequence. Possible secondary motifs are underlined [b] IC50 represents the peptide concentration that displaces half of the reference peptide. [c] *In vitro* responses were examined in subjects with established T1D. The response rate (percentage of subjects with a positive response) is noted and the fraction of responders is listed in parenthesis.

Figure 1.

a

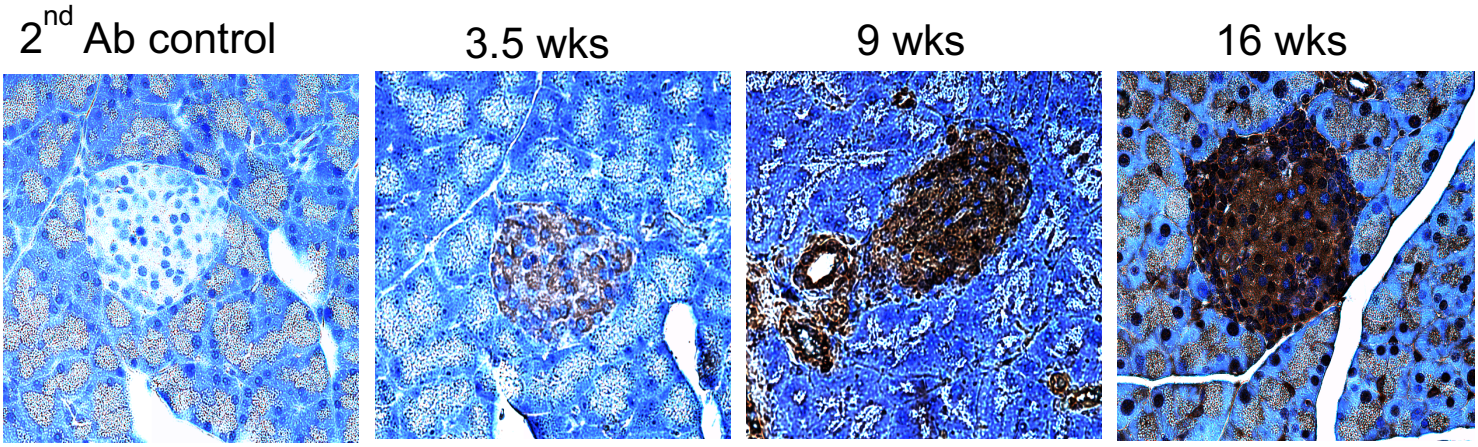

b

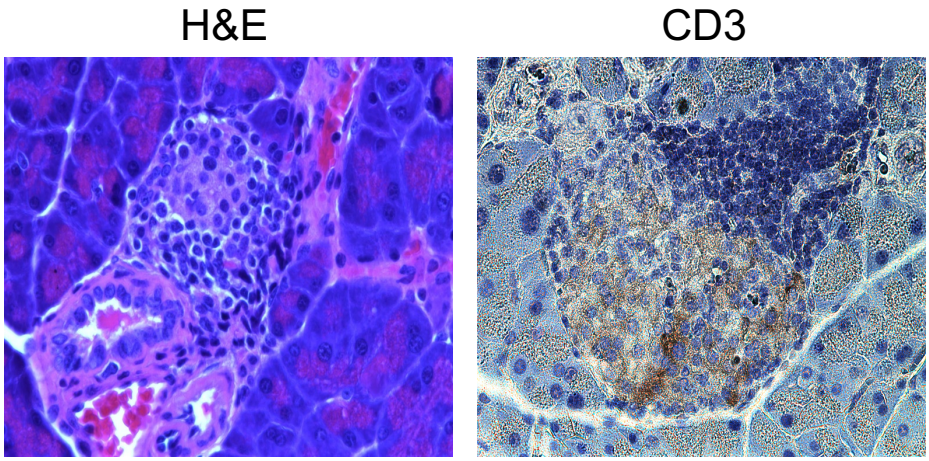

c

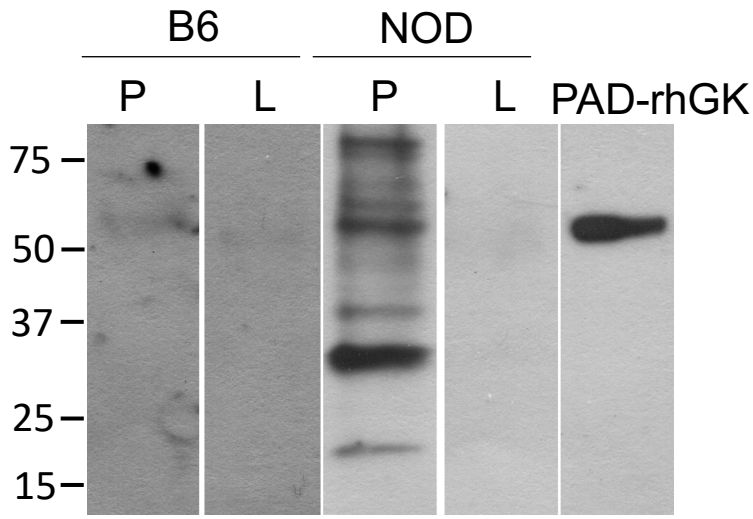

Figure 1. --continued

d

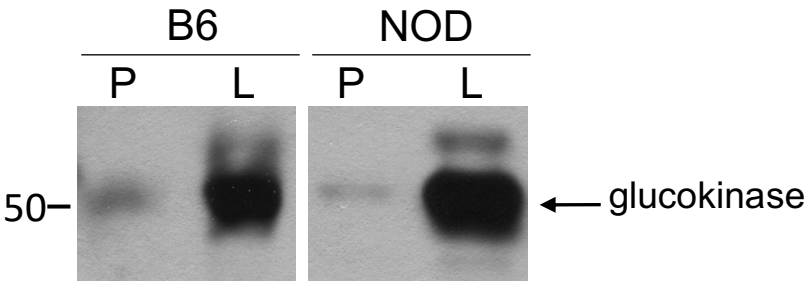

e

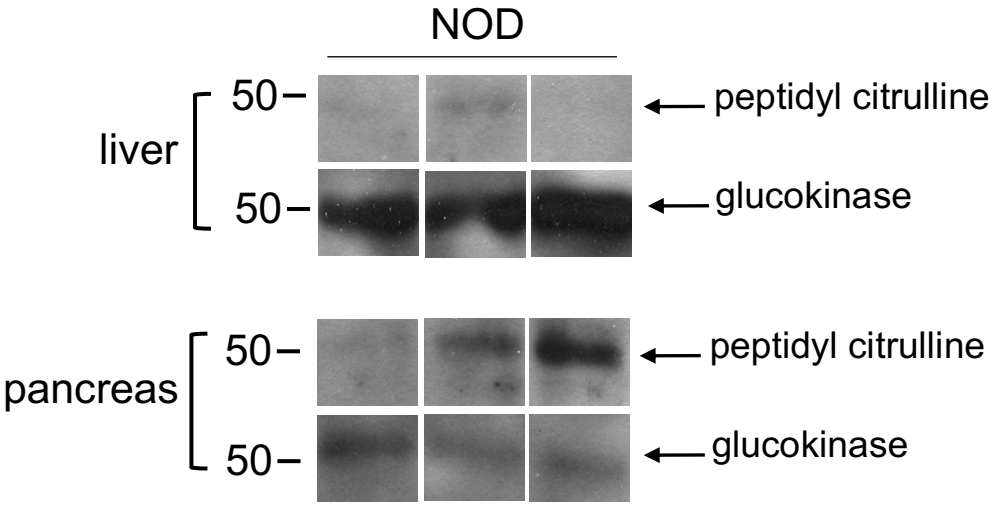

Figure 2.

a

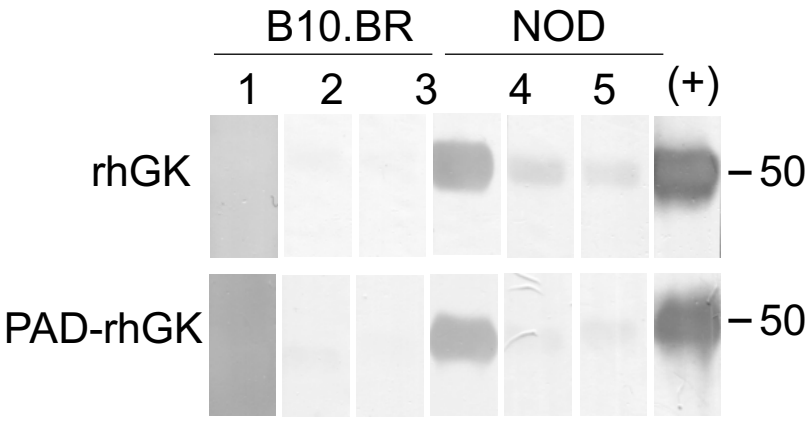

b

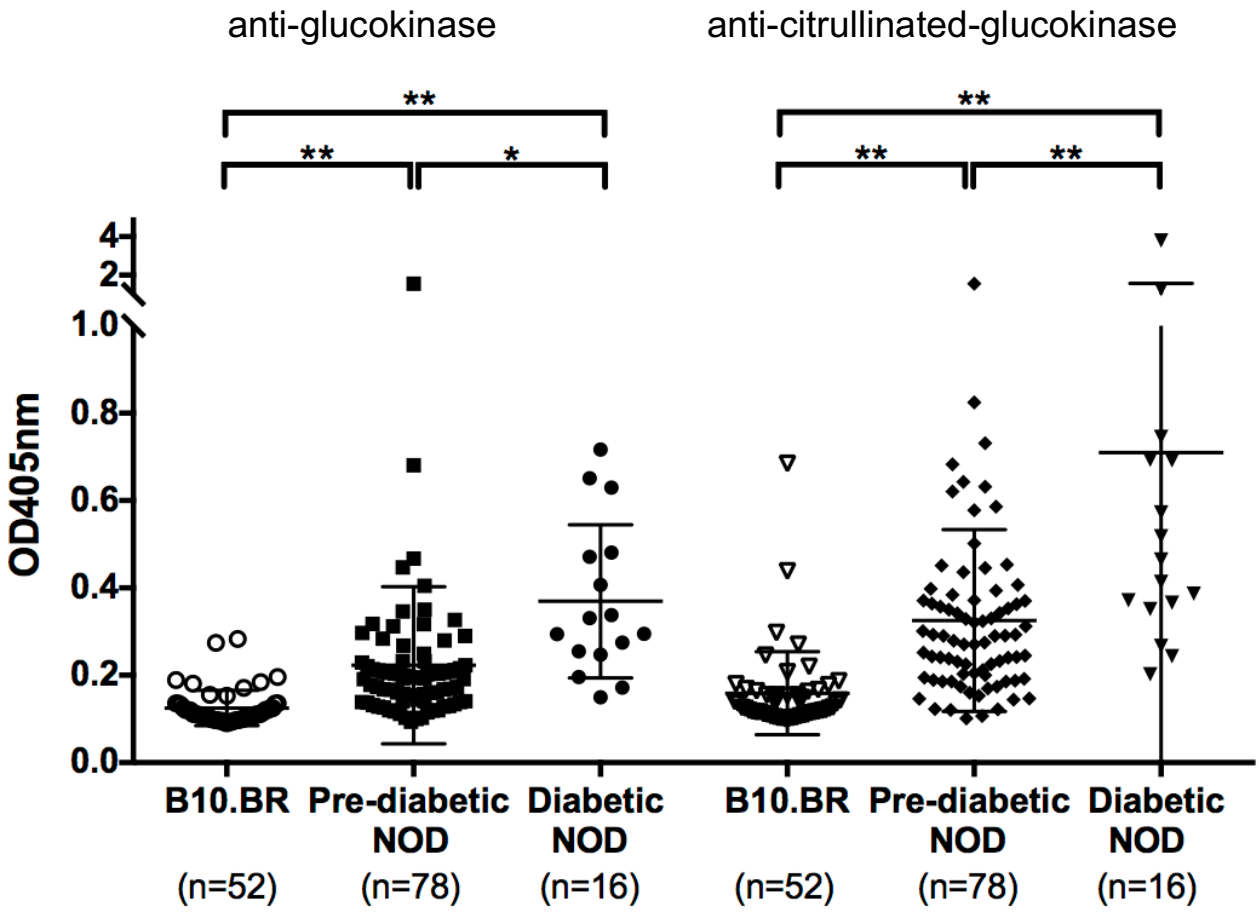

Figure 2. –continued

C

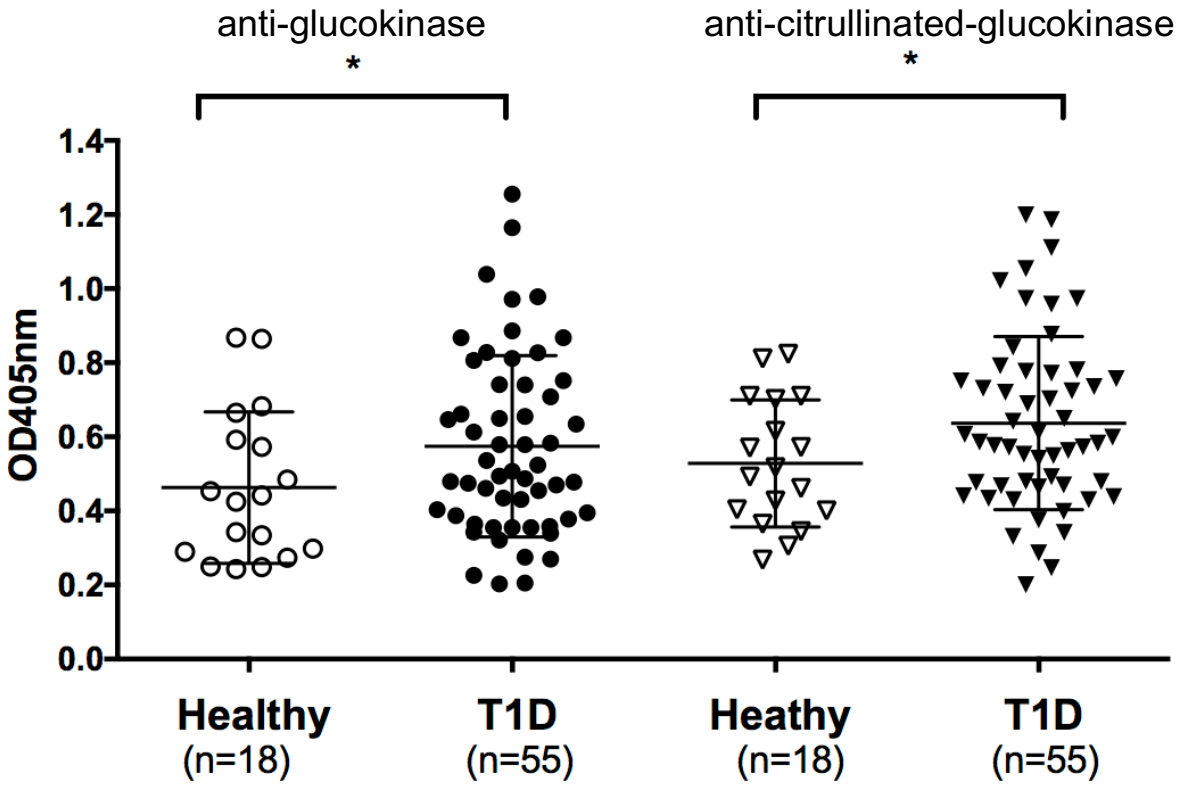

Figure 3.

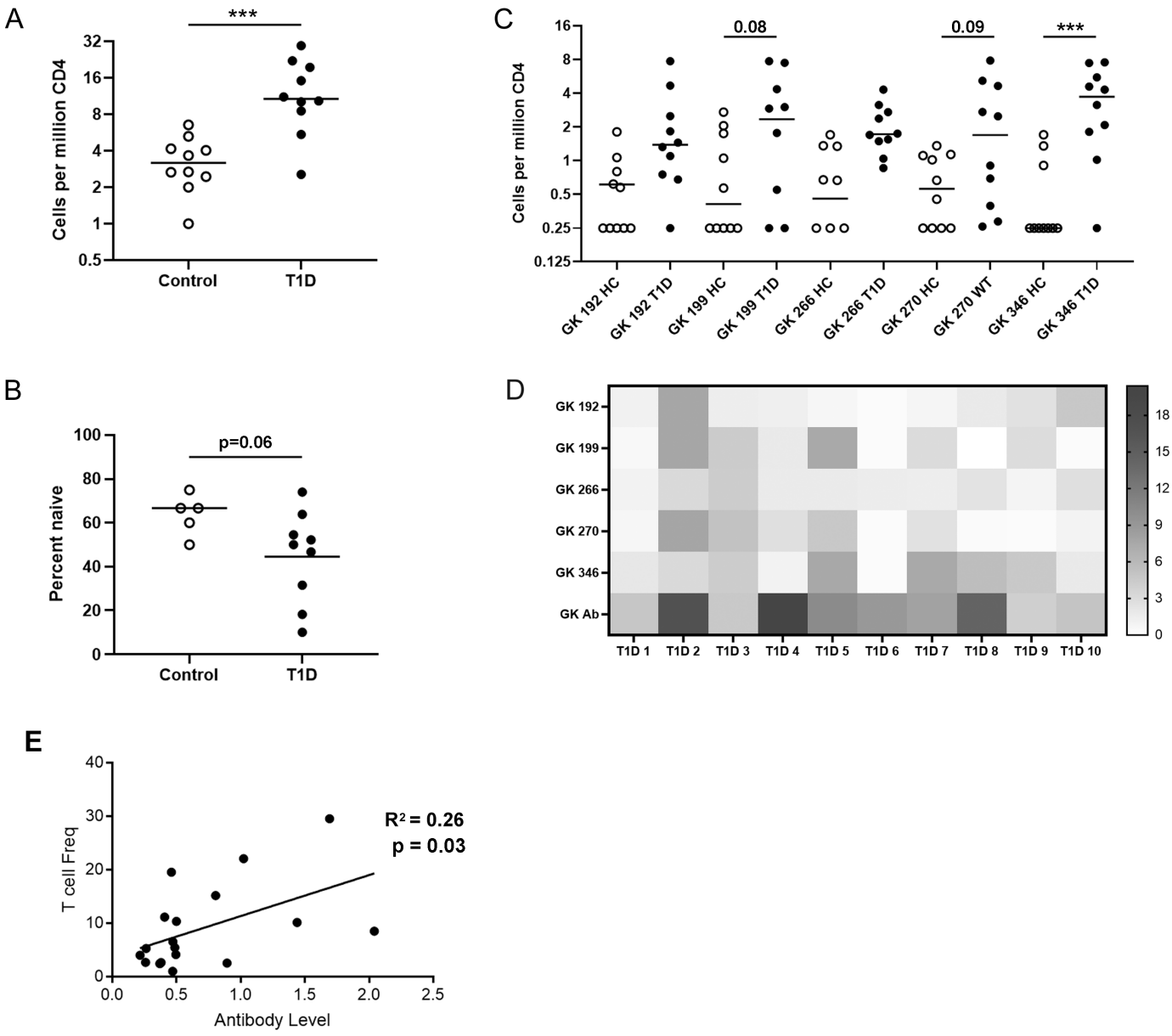

Figure 4.

a

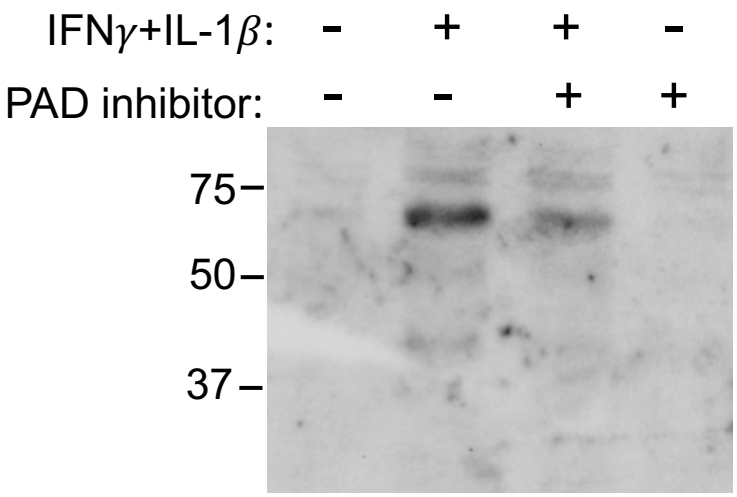

b

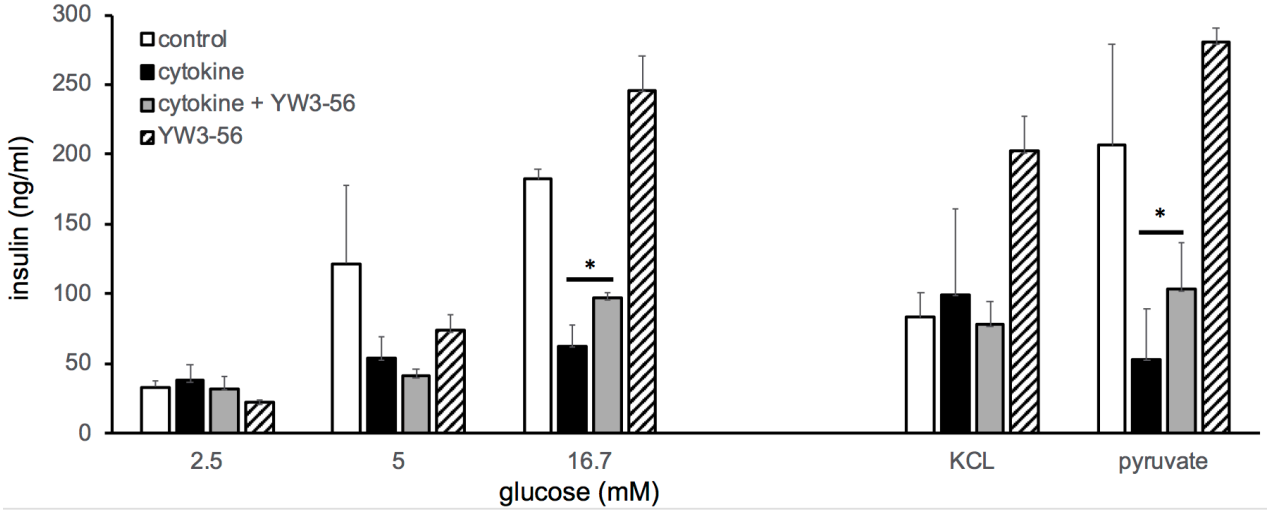

Figure 5.

a

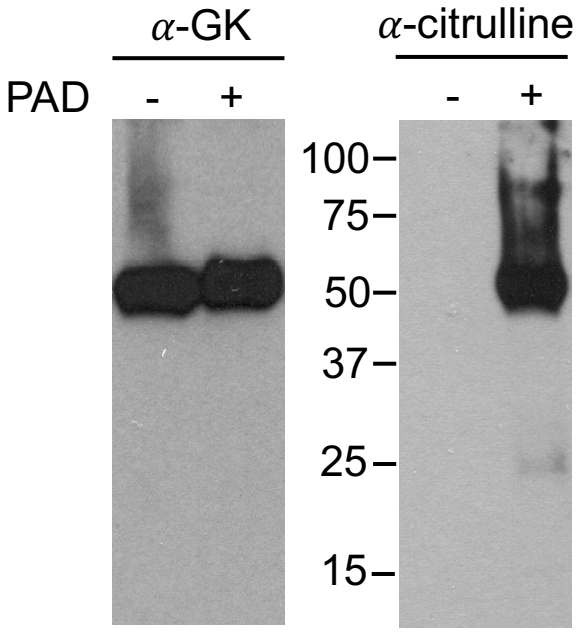

b

```
  1 mlddrarmea akkekveqil aefqlqeedl kkvmrrmqke mdrglRleth eeasvkmlpt
 61 yvrstpegse vgdflsldlg gtnfrvmlvk vgegeegqws vktkhqmysi pedamtgtae
121 mlfdyiseci sdfldkhqmk hkklplgftf sfpvrhedid kgillnwtkg fkasgaegnn
181 vvgllRdaik rrgdfemdvv amvndtvatm iscyyedhqc evgmivgtgc nacymeemqn
241 velvegdegr mcvntewgaf gdsgeldefl leydrlvdes sanpgqqlye kliggkymge
301 lvrlvllrlv denllfhgea seqlrtRgaf etRfvsqves dtgdRkqiyn ilstlglRps
361 ttdcdivRRa cesvstRaah mcsaglagvi nRmresRsed vmRitvgvdg svyklhpsfk
421 eRfhasvRRl tpsceitfie seegsgRgaa lvsavackka cmlgq
```

Figure 5. ---continued

c

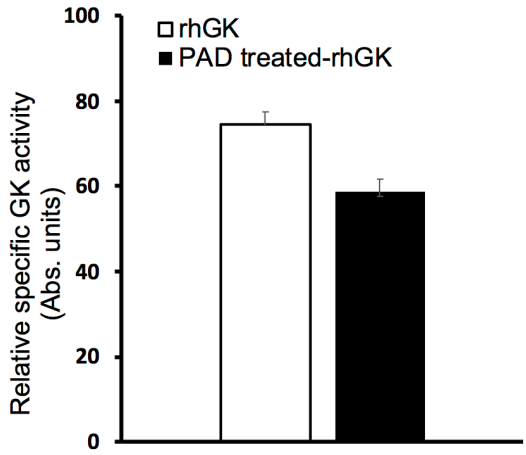

d